

# Scattering of Electron-Cyclotron waves by plasma density fluctuations in tokamaks

J. Cazabonne<sup>1</sup>, S. Coda<sup>1</sup>, J. Decker<sup>1</sup>, Y. Peysson<sup>2</sup>

<sup>1</sup> *École Polytechnique Fédérale de Lausanne (EPFL), Swiss Plasma Center (SPC), CH-1015 Lausanne, Switzerland*

<sup>2</sup> *Commissariat à l'Énergie Atomique et aux Énergie Alternatives (CEA), Institut de Recherche sur la Fusion par confinement Magnétique (IRFM), F-13108 Saint-Paul-lez-Durance, France*

Electron-Cyclotron (EC) waves in tokamak plasmas result in very efficient energy transfer from the wave to the plasma, highly localized in real and phase space [1]. Such high efficiency and accuracy make EC waves a powerful tool for Resonant Heating (ECRH), Current Drive (ECCD) and especially MHD mode mitigation, such as Neoclassical Tearing Modes, by driving local current in magnetic islands. However, it has been experimentally observed in TCV [2] and DIII-D [3] that the EC beam power deposition is broader, and current drive efficiency lower, than expected by ray tracing and drift kinetic Fokker-Planck simulations [4, 5]. Two main mechanisms have been proposed to explain this observation and both may play a significant role. The first one is an enhancement of spatial transport of fast electrons after wave absorption, leading to an *ad hoc* transport model added to drift kinetic Fokker-Planck modelling to recover experimental measurements [6], suggesting that this transport is directly proportional to the diffusion of fast electrons in both phase space and real space induced by EC waves. This has motivated the development of an ECRH operator for a gyro-kinetic code to study potential turbulent transport enhancement by EC waves from first principles [7]. The other possible cause is the average beam spatial broadening before its absorption by wave scattering due to density fluctuations, especially near the edge of the plasma. Theoretical and numerical investigations of this phenomenon have been performed with multiple approaches from ray-tracing coupled to a drift-kinetic model [8, 5] to a wave-kinetic and full-wave model [9, 10], leading to the conclusion that it can have a significant impact on EC beam broadening, particularly in the case of a long beam path before absorption. In TCV, this effect has been experimentally observed for a top-launched third-harmonic O-polarized transmitted beam, and compared with predictions, first considering only Scrape-Off-Layer turbulence from a Braginskii solver [11] and later adding core turbulence from gyro-kinetic simulations [12]. DIII-D observations on the effect of density fluctuations have also been recently reported [13]. A study of this effect in TCV for reactor-relevant conditions, i.e. Low-Field-Side-launched, fully-absorbed, second-harmonic X-polarized beam, is currently being done through preliminary numerical studies to investigate

the potential impact of density fluctuations in such a configuration; in addition, numerical tools are being set up for experimental analysis.

**Numerical tools: Ray-Tracing C3PO and 2D Full-Wave COMSOL.** C3PO is a Ray-Tracing code solving wave propagation and absorption [14], embedded in the fully relativistic bounce-averaged drift-kinetic Fokker-Planck code LUKE [15], which computes the electron distribution function. This is then used by the synthetic diagnostic R5-X2 [16] to calculate the Hard X-Ray (HXR) Bremsstrahlung emission from suprathermal electrons measured by the TCV HXR Spectrometer [17], the main tool to experimentally follow the dynamics of electrons heated by EC waves. However, C3PO relies on the WKB approximation, which requires the beam wavelength to be much shorter than the fluctuation size, which in turn has to be much smaller than the equilibrium length. On the other hand, the 2D full-wave finite-element COMSOL solver computes only the beam propagation in a cold plasma [11], but is intrinsically not limited in space scale ordering, making it a good choice for validating C3PO in a turbulent plasma.

**C3PO vs COMSOL without density fluctuations: new beam width model for C3PO.** A first benchmark of C3PO against COMSOL in a quiet plasma has led to an improved model for Gaussian beam width calculation in C3PO. This width is used to spread the power-carrying beamlets around the central ray and was initially computed assuming a Gaussian beam in vacuum. The new model is based on a chain of ray transfer matrices derived from paraxial wave equations [18], assuming a step-wise refractive index.

The ray transfer matrix for one step is given in equation 1 with  $N$  the refractive index,  $s$  the length along the central ray path and  $R_C$  the local curvature radius of the incidence interface (negative for convex surface with respect to the incoming ray, so negative for a beam entering a typical tokamak plasma). The principle is illustrated in figure 1.

$$M_{j-1 \rightarrow j} = \begin{pmatrix} 1 & ds_{j-1} \\ \frac{N_j - N_{j-1}}{N_j R_{C,j-1 \rightarrow j}} & ds_{j-1} \frac{N_j - N_{j-1}}{N_j R_{C,j-1 \rightarrow j}} + \frac{N_{j-1}}{N_j} \end{pmatrix} \quad (1)$$

Scans in averaged density, density gradient, injection poloidal angle and height for typical TCV ECRH configurations show an excellent agreement on propagation between C3PO and COMSOL (correlation over 99 % for beam position profiles). They also show a good agreement for the beam width profile (correlation over 97 %). On average, over these scans, this new model reduces the average absolute gap between C3PO and COMSOL for the beam width profile by 55 % with respect to the beam-in-vacuum model.

**Preliminary fluctuation studies with COMSOL in TCV ECRH configuration.** Numerical

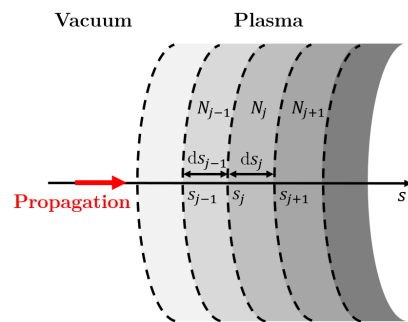


Figure 1: Principle of plasma discretization

fluctuation studies have been performed with the full-wave COMSOL model, using an analytic equilibrium [19] and analytic density fluctuations derived from a drift-wave-turbulence-based model, which consists of a superposition of independent Fourier modes [8, 5]

$$\frac{\delta n_e}{n_e} = F_\Delta F_\lambda \left( 2\pi^{1/4} \sqrt{\frac{L_f}{L_\perp}} \sigma_f \sum_{p \geq 1} \exp\left(-\frac{\pi^2}{2} p^2 \frac{L_f^2}{L_\perp^2}\right) \sin \Phi_p \right) \quad (2)$$

Where  $F_\Delta$  is a spatial Gaussian envelope centered around the Last Closed Flux Surface parametrized by its HWHM  $\Delta$ ,  $F_\lambda$  is a poloidal asymmetry for ballooning effects,  $\sigma_f$  is the standard deviation of fluctuation amplitude,  $L_f$  is the fluctuation correlation length,  $L_\perp$  is a characteristic length,  $p$  is the mode number and  $\Phi_p$  is the random Fourier phase of the mode.

Turbulence is assumed to be frozen with respect to beam propagation and the time step is chosen to exceed the fluctuation correlation time, meaning that fluctuation snapshots are independent. The beam's electric field is averaged over 100 snapshots and the transverse electric profile is studied at locations preceding the wave absorption layer. The beam profile in the turbulent plasma is mainly characterized by its FWHM normalized to the quiet plasma case. A typical configuration is depicted in figure 2.

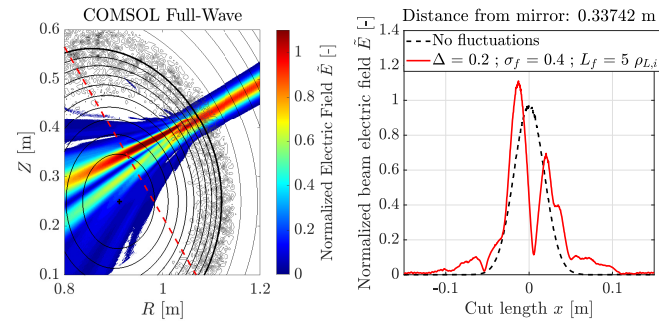


Figure 2: *Full-wave beam propagation through a turbulent plasma, for a given fluctuation snapshot and transverse beam profile taken on the dotted red line*

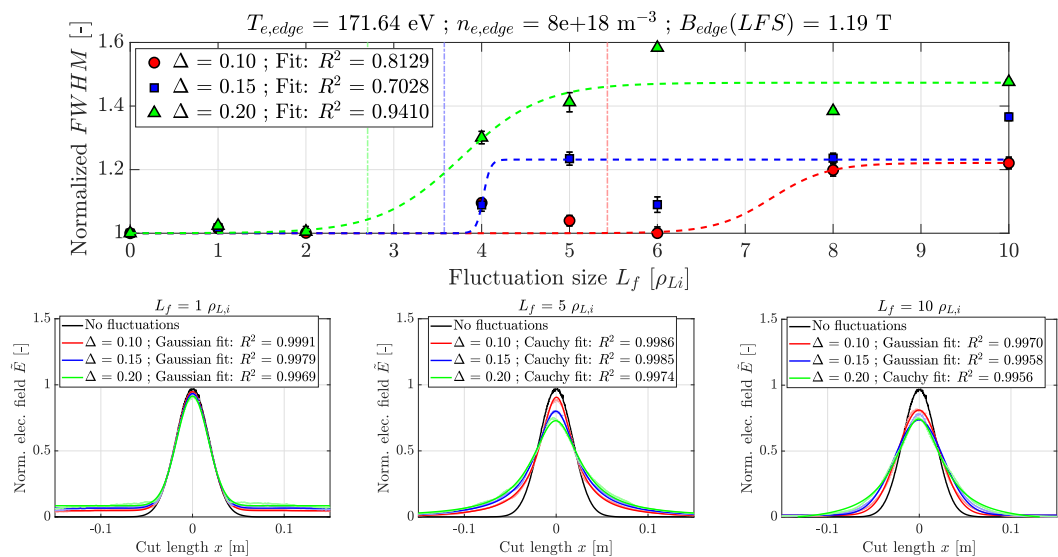


Figure 3:  *$L_f$  scans for different  $\Delta$  and given equilibrium, with examples of beam profiles*

Scans in fluctuation size ranging from 1 to 10 ion sonic Larmor radii have been done for different  $\Delta$  and edge electron density and temperature (see figure 3). The beam FWHM as a function of  $L_f$  exhibits a sudden jump that can be interpreted as a change in diffusion regime [10, 9]. For small  $L_f$ , the superdiffusive regime is characterized by a Gaussian with the addition of increasing wings. At large  $L_f$ , in the diffusive regime, the Gaussian beam significantly broadens to a saturated level. An intermediate regime can be identified, corresponding to an increase of the FWHM and a change in shape from Gaussian to Lorentzian [10]. The expected regime transition is estimated from wave kinetic theory [9] while the calculated one is given by the sigmoid fitting of FWHM vs  $L_f$ . A summary of the scans is given in figure 4. A broadening up to 50 % is observed for TCV-relevant parameters. The worst case scenario for EC power deposition accuracy corresponds to the diffusive regime, i.e., large  $L_f$ . At large  $L_f$ , the use of C3PO is expected to be valid. The level of diffusive broadening is higher for larger turbulent layer and higher edge density (and/or fluctuation amplitude). Higher temperature means larger sonic Larmor radii and so larger  $L_f$ , meaning that the diffusive regime is more easily reached. For conditions in which broadening is modest, the regime transition is less clear.

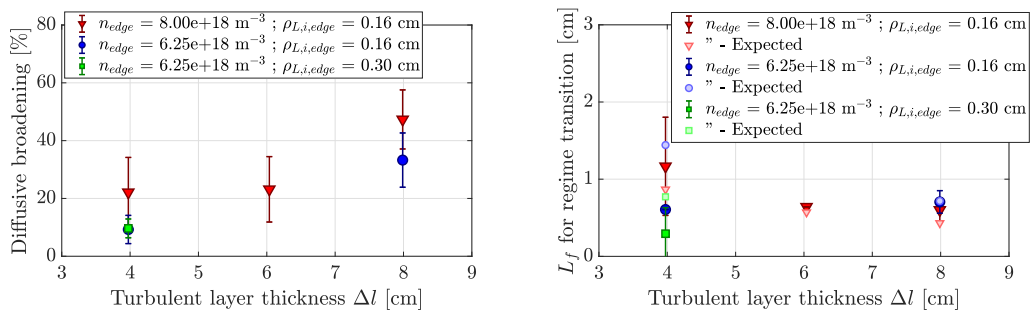


Figure 4: Results of diffusive broadening in FWHM and expected vs calculated regime transition

**Acknowledgements.** This work has been carried out within the framework of the EUROfusion Consortium and has received funding from the Euratom research and training programme 2014-2018 and 2019-2020 under grant agreement No 633053. The views and opinions expressed herein do not necessarily reflect those of the European Commission. This work was supported in part by the Swiss National Science Foundation.

## References

- [1] R. Prater, Physics of Plasmas **11**, 2349 (2004)
- [2] S. Coda *et al*, Nucl. Fusion **43**, 1361 (2003)
- [3] M. W. Brookman *et al*, EPJ Web Conf. **147**, 03001 (2017)
- [4] P. Nikkola *et al*, Nucl. Fusion **43**, 1343 (2003)
- [5] Y. Peysson *et al*, Plasma Phys. Control. Fusion **53**, 124028 (2011)
- [6] D. Choi *et al*, Plasma Phys. Control. Fusion **62**, 115012 (2020)
- [7] P. Donnel *et al*, Plasma Phys. Control. Fusion **63**, 064001 (2021)
- [8] J. Decker *et al*, EPJ Web Conf. **32**, 01016 (2012)
- [9] A. Snicker *et al*, Nucl. Fusion **58**, 016002 (2017)
- [10] A. Köhn *et al*, Plasma Phys. Control. Fusion **60**, 075006 (2018)
- [11] O. Chellaï *et al*, Plasma Phys. Control. Fusion **61**, 014001 (2018)
- [12] O. Chellaï *et al*, Nucl. Fusion **61**, 066011 (2021)
- [13] M. W. Brookman *et al*, Physics of Plasmas **28**, 042507 (2021)
- [14] Y. Peysson *et al*, Plasma Phys. Control. Fusion **54**, 045003 (2012)
- [15] Y. Peysson *et al*, Fusion Science and Technology **65**, 22 (2014)
- [16] Y. Peysson and J. Decker, Phys. Plasmas **15**, 092509 (2008)
- [17] S. Gnesin *et al*, Rev. Sci. Instrum. **79**, 10F504 (2008)
- [18] P. F. Goldsmith, *Quasioptical systems: Gaussian beam propagation and applications*, IEEE press (1998)
- [19] A. J. Cerfon and J. P. Freidberg, Physics of Plasmas **17**, 032502 (2010)